J Biol Inorg Chem (2003) 8: 689–697
DOI 10.1007/s00775-003-0468-1

ORIGINAL ARTICLE

Siucheong Yan · Fei Li · Keyang Ding · Hongzhe Sun

Reduction of pentavalent antimony by trypanothione and formation of a binary and ternary complex of antimony(III) and trypanothione

Received: 30 January 2003 / Accepted: 28 April 2003 / Published online: 21 June 2003

Abstract Several pentavalent antimony compounds have been used for the treatment of leishmaniasis for decades. However, the mechanism of these antimony drugs still remains unclear. One of their targets is thought to be trypanothione, a major low molecular mass thiol inside the parasite. We show that pentavalent antimony (Sb^V) can be rapidly reduced to its trivalent state by trypanothione at mildly acidic conditions and 310 K ($k = 4.42\ M^{-1}\ min^{-1}$ at pH 6.4), and that Sb^{III} can be bound to trypanothione to form an Sb^{III}-trypanothione complex. NMR data demonstrate that Sb^{III} binds to trypanothione at the two thiolates of the cysteine residues, and that the binding is pH dependent and is strongest at biological pH with a stability constant $\log K = 23.6$ at 298 K (0.1 M $NaNO_3$). The addition of low molecular monothiol ligands such as glutathione and cysteine to the Sb^{III}-trypanothione complex results in the formation of a ternary complex. Thiolates from both trypanothione and monothiol bind to the Sb^{III} center. The formation of the ternary complex is important, as the antileishmanial properties of the drugs are probably due to a complex between of Sb^{III}-trypanothione and enzymes. Although thermodynamically stable, the complex is kinetically labile and the free and bound forms of thiolates exchange on the ^1H NMR timescale. Such a facile exchange may be crucial for the transport of Sb^{III} within parasites.
Electronic Supplementary Material Supplementary material is available for this article if you access the article at http://dx.doi.org/10.1007/s00775-003-0468-1. A link in the frame on the left on that page takes you directly to the supplementary material.

Keywords Antimony · Electrospary ionization mass spectrometry · Nuclear magnetic resonance spectroscopy · Reduction · Trypanothione

Abbreviations amastigote: the parasites culture at pH 5.0 and 310 K to resume the intracellular form · BPR: bromopyrogallol · ESI-MS: electrospary ionization mass spectrometry · GSH: glutathione · pH^*: pH meter reading in D_2O without correction for isotope effects · promastigote: the parasites culture at pH 7.4 and 298 K to resume the extracellular stage · $T(SH)_2$: reduced form of trypanothione · T(S-S): oxidized form of trypanothione (disulfide form) · TR: trypanothione reductase · tart: tartrate

Introduction

The trypanosomatid parasite *Leishmania* causes a wide range of human diseases including kala azar and other less severe forms of leishmaniasis. Millions of people have clinical symptoms, and 400,000 new cases are reported each year [1]. Two pentavalent antimonial drugs, sodium stibogluconate (Pentostam) and meglumine antimonite (Glucantime), have been widely used for the treatment of human visceral leishmaniasis for several decades [2, 3, 4, 5]. Despite their extensive use, the mechanism of antileishmanial action, including its side effects, still remains unclear. It has been suggested that Sb^V is a prodrug and is intracellularly reduced to trivalent form (Sb^{III}), the active form of the drugs at or near the site of action. The antileishmanial activity of Sb^V has been found to be dependent on its reduction to Sb^{III} inside parasites [6]. The greater susceptibility of Sb^V to intracellular amastigotes than promastigotes suggests that the reductive activation of the drug occurs within the intracellular amastigotes. Arsenate (As^V), the analogue of antimonial, is known to be reduced to

Electronic Supplementary Material Supplementary material is available for this article if you access the article at http://dx.doi.org/10.1007/s00775-003-0468-1. A link in the frame on the left on that page takes you directly to the supplementary material.

S. Yan · F. Li · K. Ding · H. Sun (✉)
Department of Chemistry and Open Laboratory of Chemical Biology, University of Hong Kong, Pokfulam Road, Hong Kong, P.R. China
E-mail: hsun@hkucc.hku.hk
Tel.: +852-2859-8974
Fax: +852-2857-1586

arsenite (As^{III}) by arsenate reductase (e.g., ArsC and Acr2p) in yeasts, bacteria and even mammalian systems, and a mechanism for catalysis has been proposed [7, 8, 9, 10, 11, 12, 13]. Surprisingly, Sb^{V} cannot be reduced by this enzyme [14], and no analogous reductive enzyme in *Leishmania* has been identified.

Trypanothione [$T(SH)_2$], a conjugation between the tripeptide glutathione and the polyamine spermidine [i.e., N^1,N^8-bis(glutathionyl)spermidine], is the most important and abundant (>80%) low molecular mass thiol within the *Leishmania* species [15, 16, 17]. In combination with trypanothione reductase (TR), $T(SH)_2$ provides an intracellular reducing environment in parasites, in contrast to the glutathione found in mammalian systems, and is crucial for the survival of the parasites [18, 19]. $T(SH)_2$ is also involved in the detoxification of metal ions, and an ATP-coupled As^{III}/Sb^{III}-$T(S)_2$ pump (PGPA protein) has been described which extrudes the metal-(TS_2) complex from parasites [17, 20]. Overproduction of trypanothione leads to resistance to antimonials and arsenicals [21]. Trypanothione metabolism has therefore long been regarded as an attractive target in antileishmanial and antitrypanosomal drug design [22], and one of the major targets for antimonial drugs is probably $T(SH)_2$.

Low molecular mass thiols such as glutathione have already been shown to reduce antimonial and arsenate; however, this process is too slow to be biologically significant [10, 23, 24, 25, 26]. In this paper, we report an unexpectedly rapid reduction of Sb^{V} to Sb^{III} by trypanothione and then characterize the complexation of Sb^{III} to trypanothione by electrospray ionization mass spectrometry (ESI-MS) and NMR spectroscopy. The $Sb^{III}(TS_2)$ complex is thermodynamically stable but kinetically labile, and forms a ternary complex upon addition of monothiols such as cysteine and glutathione. The interaction between antimony and $T(SH)_2$ and other thiols (e.g., GSH and enzymes) may play a role in the pharmacology of antimony.

Materials and methods

Materials

Antimony trichloride (Aldrich), *N*-acetyl-L-cysteine (Sigma), oxidized trypanothione (Bachem), potassium antimony tartrate (Aldrich), reduced glutathione (GSH) (Sigma), tris(2-carboxyethyl)phosphine (TCEP) (Aldrich), 5,5′-dithiobis(2-nitrobenzoic acid) (DTNB) (Sigma), bromopyrogallol (BPR) (Sigma), dithiothreitol (DTT) (Sigma), $NaNO_3$ (99.99%, Aldrich), NaOD, DCl (Aldrich) and D_2O (Sigma), and ^{13}C-labeled cysteine (98%, Cambridge Isotope Laboratories) were used as received. Sodium stibogluconate (batch GW387208A) was provided by GlaxoWellcome (Stevenage, UK).

Sample preparation

In all experiments, the concentration of reduced trypanothione was determined by titration with DTNB [27]. ESI-MS experiments were carried out in a solution of $SbCl_3$ and $T(SH)_2$. Other ligands such as tartrate and citrate used in the experiments were prepared from tartaric acid and citric acid using 1 M ammonia for pH adjustment. All the samples were adjusted to pH≈7 by ammonia.

NMR experiments were carried out in D_2O or H_2O/D_2O (90/10) in the presence of 10 mM phosphate buffer. Solutions containing 5 mM of antimony complexes and various ratios of $T(SH)_2$ were used in the experiments. Adjustment of pH* was made with NaOD and the solutions were then exposed to nitrogen (99.9%) for at least 10 min to minimize the oxidation of $T(SH)_2$. All solutions used for the study of formation constants contained 5 mM Sb^{III}(tart), 5 mM $T(SH)_2$ and 0.1 M $NaNO_3$ in D_2O. Measurements of pH* were made with a Corning 440 pH meter equipped with a micro combination electrode (Aldrich), calibrated with standard buffer solutions. The meter readings for D_2O solutions were recorded as pH* values without correction for isotope effects.

Electronic absorption spectroscopy studies were carried out in a solution containing 1 mM Sb^{V}(gluconate) and 2 mM $T(SH)_2$ in the presence of 10 mM phosphate buffer at different pH values. In the kinetics studies, the analytical solutions were kept under a nitrogen atmosphere to minimize the oxidation of $T(SH)_2$.

Electronic absorption spectroscopy

Determination of the Sb^{III} content was carried out on a Varian Cary 50 UV-vis spectrometer, as described previously [23]. A solution containing 700 μL of 15 μM bromopyrogallol (BPR) was used for Sb^{III} detection. Aliquots of the sample solution (5–20 μL) were added to the BPR cuvette. Sb^{III} tartrate was used as a standard. The absorbance of BPR at 560 nm decreased proportionally to the amount of Sb^{III} in the medium, and a calibration curve was generated for calculating the Sb^{III} concentration. We checked that neither Sb^{V} nor $T(SH)_2$ (and GSH) in the analyte solution interfered with the colorimetric test. For kinetics studies of Sb^{V} reduction, aliquots of the sample were added to the BPR-containing cuvette to monitor the Sb^{III} formation profile. The rate of reduction (k) was calculated from a non-linear square fit of the data by assuming a second-order reaction between Sb^{V} and $T(SH)_2$.

NMR experiments

All ^{1}H NMR experiments were carried out on Bruker DRX500 and AV600 spectrometers at 278–298 K. Typical acquisition conditions for ^{1}H NMR were 45° pulse length (5 μs), 2.0 s relaxation delay (4 s for determination of formation constants), 16k data points and 16–32 transients. Spectra were processed using an exponential function with a line-broadening coefficient of 0.3 Hz. Standard TOCSY, NOESY and ROESY pulse sequences were used with a spectrum width of 10 ppm and a relaxation delay of 2–4 s. Several mixing times were chosen in the range of 20–75 ms (2D TOCSY), 200–400 ms (2D NOESY) and 150 ms (2D ROESY) respectively, with 2k data points in the t_2 dimension and 256 increments in the t_1 dimension. The spectra were zero-filled to a 2k×1k matrix. The standard NOESY pulse sequence was used to perform the 2D exchange spectroscopy (EXSY). A 1D heteronuclear single-quantum coherence spectrum (HSQC or ^{13}C edited ^{1}H NMR spectrum) was recorded using the first increment of the 2D HSQC sequence. In all experiments, the solvent resonance (residual water) was suppressed via presaturation during the relaxation delay, and the resonance of the water signal for experiments performed in H_2O/D_2O (90/10) was suppressed by the WATERGATE pulsed-field-gradient sequence [28].

Electrospray ionization mass spectrometry

Positive ion electrospray mass spectrometry was performed on an LCQ spectrometer (Finnigan). The sample was infused at 3 μL min^{-1} and the ions produced in an atmospheric pressure

ionization (API)/ESI ion source. The source temperature was 453–473 K and the drying gas flow rate was 0.9 L min^{-1}. A potential of 3.5 kV was applied to the probe tip, and a cone voltage of −10 V over 200–2000 Da was used. The quadrupole was scanned at 100 amu s^{-1}. The mass accuracy of all measurements was within 0.5 *m/z* units. The acquisition and data processes were performed on a Microsoft Windows NT operating system.

Preparative HPLC separations of trypanothione

Reduced trypanothione was separated by a cation-exchange column (a preparative MN-nucleosil 100-10 SA column, pore size 100 Å, particle size 10 µm) equipped with a Waters 510 HPLC pump and a Waters 410 differential refractometer as the detector. Isocratic elution (8 mL min^{-1}) of 1 M KNO_3 was applied as a solvent system. After initial separation by the cation-exchange column, the fraction containing trypanothione was freeze-dried and redissolved in a minimum amount of the mobile phase as described below and then desalted by a GL Science Intertsil PREP ODS reverse-phase column (pore size 100 Å, particle size 10 µm). Isocratic elution (8 mL min^{-1}) with 10 mM $NaClO_4$ and 0.1% v/v of 85% H_3PO4 was applied.

Results

HPLC separation of trypanothione

The reduced form of trypanothione [$T(SH)_2$] was obtained via reduction of its oxidized form [T(S-S)] using tris(2-carboxyethyl)phosphine (TCEP) [29], and was further purified by HPLC. Since trypanothione has a very strong ion-pair interaction with the stationary phase (sulfonate group) via the spermidine amine group, a higher ionic strength mobile phase (1 M KNO_3) was used to elute trypanothione from the column. Reduced [T(S-S)] and oxidized trypanothione [$T(SH)_2$] were eluted at 19 and 20 min, respectively, while TCEP was eluted at 10 min (Fig. 1). After the fraction containing trypanothione was collected, it was freeze-dried and desalted as described (Materials and methods), to produce an appropriate ionic strength for NMR experiments.

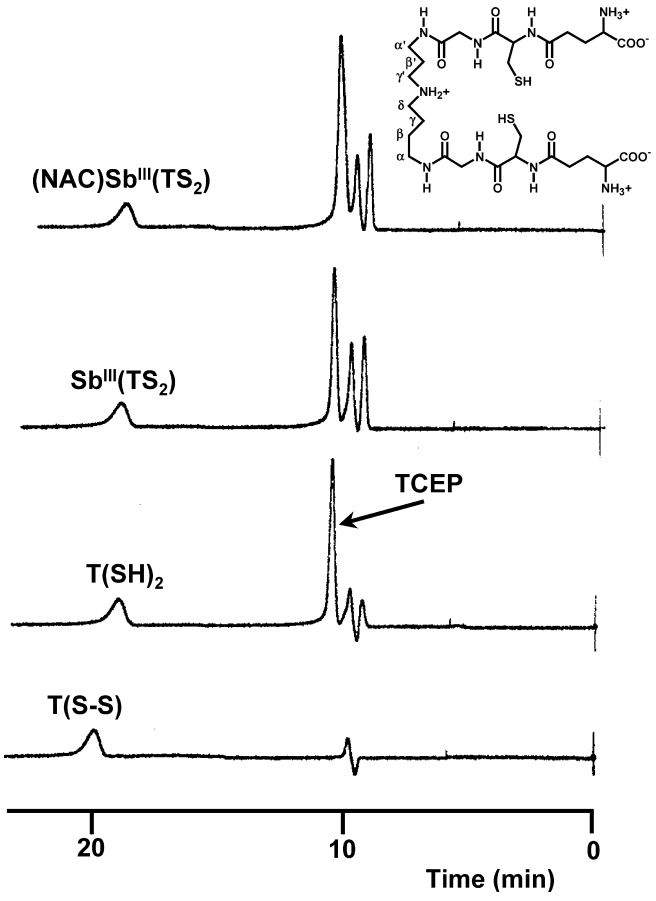

Fig. 1 HPLC profile of the separation of reduced trypanothione [$T(SH)_2$], oxidized trypanothione [T(S-S)], (NAC)$Sb^{III}(TS_2)$ and tris(2-carboxyethyl) phosphine (TCEP). *Insert*: structure of $T(SH)_2$

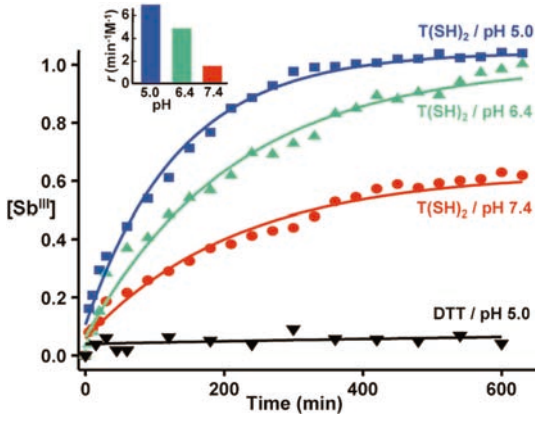

Fig. 2 Kinetics of the reduction of Sb^V in aqueous solution at pH 5.0, 6.4 and 7.4 and 310 K by $T(SH)_2$ or DTT. The *insert* is the rate of reduction by $T(SH)_2$ at 310 K and different pH values; simulation of the reaction rate is described in Materials and methods. The solution was maintained in a nitrogen atmosphere

Reduction of Sb^V complex by reduced trypanothione

UV-vis spectroscopy was used to investigate the reduction of antimony(V) by trypanothione with bromopyrogallol (BPR) as indicator. When $T(SH)_2$ was incubated with Sb^V (as sodium stibogluconate) in the molar ratio of 2:1 at pH 5.0 and 310 K, a gradual decrease in absorption at 560 nm was observed, indicative of the reduction of Sb^V to Sb^{III} [30]. These changes can be converted to the increase in the concentration of Sb^{III} (Fig. 2). The concentration of Sb^{III} increased exponentially and the rate of reduction of Sb^V (or formation of Sb^{III}) was calculated at 6.82 M^{-1} min^{-1} with $t_{1/2} = 73 \pm 5$ min. A slower reduction rate was observed when the sample was incubated at the higher pH of 6.4 and 7.4 (4.42 and 1.53 M^{-1} min^{-1}, respectively), showing that the rate of reduction was pH-dependent and favored under acidic pH. The rate of formation of Sb^{III} was much slower (1.66 M^{-1} min^{-1}) at the lower temperature of 298 K (pH 5.0), with $t_{1/2} = 300 \pm 5$ min. Little Sb^{III} was detected when Sb^V was incubated in the

absence of reduced trypanothione. This result indicated that $T(SH)_2$ plays a significant role in the reduction of Sb^V to Sb^{III}. For comparison, dithiothreitol (DTT), $E°_{1/2} = -0.330$ V [vs. −0.242 V for $T(SH)_2$], also a dithiol [17], was tested for its ability to reduce Sb^V to Sb^{III}. A very slow reduction process for DTT was observed under identical conditions, in contrast to the effects achieved with $T(SH)_2$ (Fig. 2).

Formation of a binary and novel ternary complex

Following the reduction of Sb^V to Sb^{III}, a complex of Sb^{III} with $T(SH)_2$ may form. Owing to the presence of potassium in the Sb^{III} tartrate complex, which greatly suppresses the ionization of the ions and results in dramatic loss of ESI-MS sensitivity, antimony trichloride ($SbCl_3$) was used in our study. In the ESI-MS spectrum of $T(SH)_2$ at pH≈7, there was a cluster of ions at *m/z* 724.9, corresponding to $C_{27}H_{50}N_9O_{10}S_2$ (calcd 724.3). A mixture of $SbCl_3$ and $T(SH)_2$ (1:1 molar ratio) at pH 7.4 gave a prominent cluster of ions related to the natural isotopic distribution of Sb (^{121}Sb:$^{123}Sb = 57:43$), with predominant peaks [M^+] at *m/z* 842.3 and 844.3 (intensity ratio 5.5:4.5), which can be assigned to $Sb^{III}(TS_2)$ (**1**, $C_{27}H_{48}N_9O_{10}S_2Sb$, calcd 843.2 and 845.2). The minor peaks at *m/z* 843.6, 845.6, 846.6 and 847.6 were due to the isotopic distribution of ^{13}C, and the distribution pattern of Sb and C agreed well with the simulations (Fig. 3A, insert). A minor cluster of ions at *m/z* 1567.2 and 1569.3 corresponded to $Sb^{III}(TS_2)_2$ complexes ($C_{54}H_{97}N_{18}O_{20}S_4Sb$, calcd 1566.5 and 1568.5). There were no further changes after addition of total 1.5 and 2 mol equiv of $T(SH)_2$ to the mixture, except an increase in the intensity of the peak at *m/z* 724.9, arising from $T(SH)_2$.

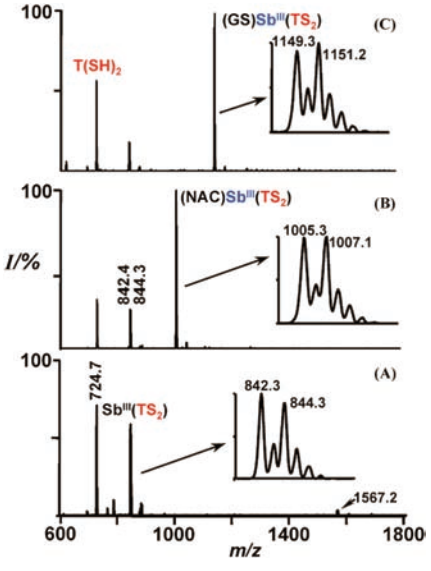

Fig. 3 ESI-MS spectra of **A** $Sb^{III}(TS_2)$ (**1**), **B** after addition of *N*-acetyl-L-cysteine and **C** glutathione. Note the new clusters formed at the larger *m/z*, indicative of formation of a ternary complex

Interestingly, the addition of one mol equiv of *N*-acetyl-L-cysteine (NAC) to **1** at the same pH value resulted in a new major cluster of ions at *m/z* 1005.3 and 1007.1 with an intensity ratio of about 5:5 in the ESI-MS spectrum, corresponding to a new complex $(NAC)Sb^{III}(TS_2)$ ($C_{32}H_{56}N_{10}O_{13}S_3Sb$, calcd 1005.4 and 1007.4 with intensity ratio 57:43) (Fig. 3B). No other major changes were observed after the further addition of NAC. Similarly, the addition of one mol equiv of the tripeptide glutathione (GSH) to **1** led to a major cluster of ions at *m/z* 1149.3 and 1151.2 with an intensity ratio 4.5:5.5, respectively. The cluster can be assigned to a ternary complex $(GS)Sb^{III}(TS_2)$ ($C_{37}H_{64}N_{12}O_{16}S_3Sb$, calcd 1149.5 and 1151.5 with intensity ratio 57:43) due to GSH binding to **1** (Fig. 3C). Again, the further addition of GSH did not produce any significant changes in the spectrum.

In order to investigate whether the formation of the ternary complex depends on the binary complex, we first incubated $SbCl_3$ with NAC at pH 7.4 for 1 h at room temperature to obtain an $Sb^{III}(NAC)_3$ complex which gave a prominent cluster [M^+] at *m/z* 607.5 and 609.1 in the ESI-MS spectrum. After addition of one mol equiv of $T(SH)_2$ to the reaction mixture, a predominant cluster of ions [M^+] at *m/z* 1005.3 and 1007.1 was observed with an intensity ratio of about 5:5, corresponding to the ternary complex $(NAC)Sb^{III}(TS_2)$. The intensity of the peaks at *m/z* 607.5 and 609.1 decreased dramatically. Only a very weak cluster at *m/z* 842.6 and 844.3 was noticed (data not shown). Similarly, after the addition of $T(SH)_2$ to the $Sb^{III}(GS)_3$ solution, a prominent cluster [M^+] at *m/z* 1149.3 and 1151.2 appeared at the expense of the initial major cluster [M^+] at *m/z* 1039.3 and 1042.1. These two groups of clusters corresponded to $(GS)Sb^{III}(TS_2)$ (calcd 1149.5 and 1151.5) and $Sb^{III}(GS)_3$ (calcd 1039.1 and 1041.1), respectively.

Other non-thiolate ligands such as tartrate or citrate were also added to $Sb^{III}(TS_2)$ solution. Little change was observed on addition of one mole equivalent of either tartrate or citrate (pH 7.4), except for the original signal at *m/z* 842.3 and 844.3 corresponding to **1**.

Thermodynamics and kinetics study of the binary and ternary complex by ^1H NMR

Sb^{III} binding to $T(SH)_2$

Trypanothione is a polydentate ligand including four carboxylate groups, two thiol groups and several amino groups. ^1H NMR spectroscopy was used to identify the target sites of Sb^{III} binding. Only one set of resonances from like residues was observed, despite the asymmetry of the sperimidine moiety. This indicates an approximate symmetry of the two halves of $T(SH)_2$, which is similar to its T(S-S) oxidized form [31]. In aqueous solution containing a $T(SH)_2$ and Sb^{III} tartrate mixture

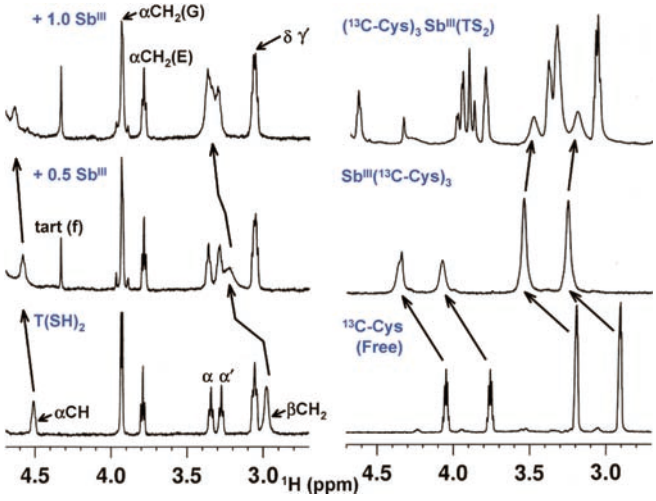

Fig. 4 ^{1}H NMR spectra of $Sb^{III}(TS_2)$ and (^{13}C-Cys)$Sb^{III}(TS_2)$ complexes. *Left*: ^{1}H NMR spectra of reduced-trypanothione [$T(SH)_2$] (*bottom*), after addition of 0.5 (*middle*) and 1 mol equiv of Sb^{III} to $T(SH)_2$ (*top*). *Right*: ^{1}H NMR spectrum of free ^{13}C-labeled cysteine (^{13}C-Cys) (*bottom*), $Sb^{III}(^{13}C\text{-}Cys)_3$ (*middle*) and the ternary complex (^{13}C-Cys)$Sb^{III}(TS_2)$ (*top*). The spectra were acquired at pH* 7.4 and 298 K

(1:1 mol ratio) at 298 K and pH* 7.4, the major changes in the spectrum were the disappearance of the resonances of the α and β protons of Cys of $T(SH)_2$, and the appearance of relatively broad resonances for these protons at a relatively lower field, as well as a new singlet which appeared at 4.33 ppm (Fig. 4).

The ^{1}H NMR spectra of free $T(SH)_2$ and $T(SH)_2$ in the presence of 0.5 and 1.0 mol equiv of Sb^{III}(tart) at pH* 7.4 are shown in Fig. 4. Reaction of $T(SH)_2$ with 0.5 mol equiv of Sb^{III} at pH* 7.4 led to the appearance of new $T(SH)_2$ peaks at 3.22 and 4.58 ppm, while the Cys βCH_2 and αCH of free $T(SH)_2$ at 2.98 and 4.51 ppm disappeared. A 2D TOCSY spectrum confirmed that the peaks at 2.98 and 4.51 ppm were coupled each other, as were the resonances at 3.22 and 4.58 ppm (data not shown). These can therefore be assigned to the βCH_2 and αCH protons of the Cys residues of the free $T(SH)_2$ and Sb^{III}-bound trypanothione, respectively.

The further addition of 0.5 mol equiv of Sb^{III} (total 1.0 mol equiv) to the $T(SH)_2$ solution produced further shifts in the resonances at 3.22 to 3.36 ppm (βCH_2) and the resonances at 4.58 to 4.64 ppm (αCH). Simultaneously, the intensity of the resonances of free tartrate at 4.33 ppm increased by 40%. No other evident changes in the proton signals of trypanothione were observed. The addition of another mol equiv of Sb^{III} resulted in little changes in the resonances except for a new resonance at 4.72 ppm, which can be assigned to the bound form of tartrate. This suggests the formation of a stable $Sb^{III}(TS_2)$ complex, which matches the ESI-MS data. The large changes in peaks for the βCH_2 and αCH of the Cys residues of $T(SH)_2$ ($\Delta\delta = 0.38$ and 0.13 ppm) suggest that thiolate groups of Cys are the binding sites for Sb^{III}.

Table 1 Chemical shifts of ^{13}C-labeled cysteine

Protons	Bound (ppm)	Free (ppm)	$\Delta\delta$ (ppm)
β-CH_2	3.15	2.90	0.25
β'-CH_2	3.43	3.18	0.25
$^1J_{CH}$	142 Hz		
α-CH	3.98	3.75	0.23
α′-CH	4.28	4.05	0.23
$^1J_{CH}$	145 Hz		

Characterization of an Sb^{III} ternary complex by ^{13}C-labeled cysteine

Because the ^{1}H NMR resonances of cysteine (and GSH) overlap with cysteine residues from trypanothione, it is difficult to distinguish whether the resonances come from cysteine or a cysteine residue from GSH or $T(SH)_2$. We therefore employed ^{13}C-labeled cysteine in this study. As the α and β protons of the cysteine were coupled with the labeled ^{13}C, a splitting ($^1J_{CH} = 145$ Hz) for both protons was observed, which allowed us to readily distinguish the resonance of ^{13}C-cysteine from GSH and trypanothione.

Figure 4 shows the ^{1}H NMR spectra of the free ^{13}C-labeled cysteine and ^{13}C-labeled cysteine (^{13}C-Cys) in the presence of 3 mol equiv of Sb^{III} tartrate or 1 mol equiv of $Sb^{III}(TS_2)$ (**1**) at pH* 7.4. Addition of 1.0 mol equiv of ^{13}C-labeled cysteine to **1** at pH* 7.4 led to resonances at 3.15 and 3.43 ppm due to ^{13}C and ^{1}H coupling ($^1J_{CH} = 142$ Hz), as well as another set of broad peaks at 3.98 and 4.28 ppm ($^1J_{CH} = 145$ Hz). A ^{13}C-edited ^{1}H spectrum shows only two resonances at 3.08 and 2.99 ppm (βCH_2), and 3.97 ppm (αCH, data not shown), which confirmed that these splittings resulted from the coupling between the carbon of $^{13}CH_2$ of Cys with its attached protons. Resonances of the β and α protons of free ^{13}C-Cys at the same pH value appeared at 2.90 and 3.18 ppm, and 3.75 and 4.05 ppm, respectively. None of the other parts of the resonance of bound trypanothione was affected by the addition of ^{13}C-Cys. Details of the assignments are listed in Table 1. The large low-field shifts of the resonances for the α and β protons ($\Delta\delta = 0.23$ and 0.25 ppm) of ^{13}C-Cys suggested that the thiolate sulfur of cysteine coordinated to the Sb^{III} center.

Both NOESY and ROESY experiments of the ternary complex (as ^{13}C-labeled cysteine) with different mixing time were performed. However, few NOE or ROE cross-peaks were observed between protons of trypanothione and those of ^{13}C-Cys, probably due to the flexible structure of the complex in the solution.

The exchange behavior of thiolate groups between free and bound forms of $T(SH)_2$ in **1** was investigated by 2D ^{1}H exchange spectroscopy (EXSY). A 2D EXSY spectrum (mixing time 400 ms) of $Sb^{III}(TS_2)$ at pH* 4 showed cross-peaks at 3.39/2.98 ppm and 4.64/4.51 ppm, which are assignable to Cys β and α protons exchange between free and bound forms of $T(SH)_2$ on

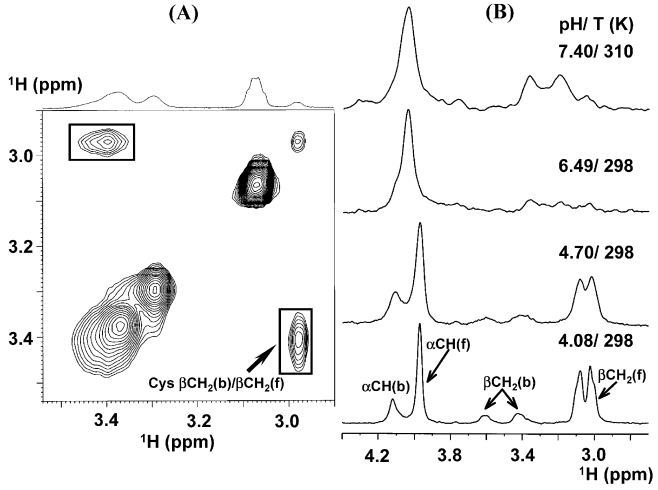

Fig. 5A, B Exchange of trypanothione between bound and free forms, and exchange of ^{13}C-labeled cysteine between its bound and free forms in the ternary complex. **A** 2D EXSY spectrum (mixing time 500 ms) of Sb^{III} in the presence of $T(SH)_2$ at pH 4.0, showing the cross-peaks for exchange between bound and free $T(SH)_2$ at 3.36/2.98 ppm. **B** ^{13}C-edited ^{1}H NMR spectrum of a solution containing 5 mM Sb^{III} in the presence of $T(SH)_2$ and ^{13}C-labeled cysteine at a mole ratio of Sb^{III}:$T(SH)_2$:^{13}C-labeled cysteine = 1:1:2 at pH 4.1–7.4 at 298 and 310 K, showing the broadening and coalescence of free and bound ^{13}C-labeled cysteine at 3.97/4.12 ppm (αCH) and 3.09, 3.10/3.42, 3.61 ppm (βCH_2) as the pH increases

the ^{1}H NMR timescale (Fig. 5A and Fig. S1). Similarly, another set of cross-peaks at 4.70/4.33 ppm was observed, due to the exchange between free and bound forms of tartrate (Fig. S1).

The exchange behavior of cysteine between free and bound forms in the ternary complex was investigated by the ^{13}C-edited ^{1}H NMR technique (1D-HSQC). A solution containing Sb^{III}, $T(SH)_2$ and ^{13}C-Cys with the ratio 1:1: 2 was used to study the exchange behavior at various pH values. At pH 4.08 and 298 K, separate resonances of free and bound forms of αCH (3.97/4.12 ppm) and βCH_2 (3.09, 3.10/3.42, 3.61 ppm) of ^{13}C-Cys were observed (Fig. 5B). As the pH was increased to 6.49, both the free and bound resonances broadened and gradually coalesced. At pH 7.40 and 310 K, only an average resonance was observed, indicative of a rapid exchange between free and bound forms of ^{13}C-labeled Cys in the ternary complex. The rate of exchange was estimated at 5–10 s^{-1} at pH^* 4.1–4.7, 298 K and $> 500\ s^{-1}$ at pH^* 7.40 and 310 K, based on previous calculations [32]. No detailed lineshape analysis was attempted due to the presence of a pH-dependent equilibrium of the ternary complex.

pH dependence of $Sb^{III}(TS_2)$

To investigate the pH^* stability of **1**, ^{1}H NMR spectra of $T(SH)_2$ and Sb^{III} tartrate at a 1:1 mol ratio were recorded over the pH range 2–9 at 298 K. At pH^* 2.4, both free and bound forms of Cys βCH_2 at 2.98 and 3.36 ppm, and αCH at 4.51 and 4.68 ppm, were observed, respectively (Fig. S2), as were the free and bound forms of tartrate at 4.62 and 4.70 ppm. Both βCH_2 and αCH resonances of free Cys decreased in intensity with the increase in pH^* value, while an increase in intensity of the bound form was observed. Simultaneously a new resonance appeared at 4.62 ppm and later shifted to 4.33 at $pH^* > 4.2$. At pH^* 7.4, the free Cys βCH_2 and αCH resonances at 2.98 and 4.51 ppm completely disappeared, and the intensity of the resonance at 4.33 ppm reached its maximum. The chemical shifts of peaks at 4.68 and 3.36 ppm were almost independent of pH^* up to 8.6, while the chemical shifts of Glu and Gly residues of $[Sb^{III}(TS_2)]$ were almost the same as those in free $T(SH)_2$, suggesting that Sb^{III} binds to $T(SH)_2$ only at the thiolate sulfur of Cys when forming an $[Sb^{III}(TS_2)]$ complex.

Table 2 Stability constants (K) for reaction between antimony tartrate and 1 mol equiv of $T(SH)_2$ at different pH* values, conditional stability constants for $Sb(TS_2)$ ($K'_{Sb(TS_2)}$) and derived stability constants ($K_{Sb(TS_2)}$) at 298 K

pH^*	log K	log $K'_{Sb(TS_2)}$	log $K_{Sb(TS_2)}$
5.5	5.76	20.6	23.5
5.0	4.78	19.6	23.1
4.5	4.36	19.2	23.1
4.0	3.95	18.8	23.2
3.5	3.74	18.6	23.5
3.0	3.71	18.5	24.0
2.5	3.80	18.6	24.6
			Average = 23.6 ± 0.4

Determination of the stability constant for $[Sb^{III}(TS_2)]$

A reversible reaction was observed between Sb^{III} tartrate and $T(SH)_2$. At low pH^* values, Sb^{III} binds strongly to tartrate, whereas at higher pH^* values, $T(SH)_2$ displaces tartrate gradually. The stability constants can therefore be calculated, based on the integration of free and bound βCH_2 of Cys (Table 2), with the following procedures. We consider Sb(tart) as a monomer, although it is a dimer in the solid state [33]. An equilibration reaction occurs in aqueous solution between the monomer and dimer, and at higher pH values, and an ionic strength of 0.1 M, most of this compound will be present as monomers. Firstly, the pH^*-dependent stability constant (K) is determined at different pH^* values by integration of the appropriate ^{1}H NMR peaks:

$$[Sb(tart)^-] + TS_{2(t)} \rightarrow [Sb(TS_2)] + tart^{4-}$$

$$K = \frac{[Sb(TS_2)][tart^{4-}]}{[Sb(tart)^-][TS_2]_{(t)}} \quad (1)$$

where $TS_{2(t)}$ is the total free trypanothione, i.e. $[TS_2]_{(t)} = [TS_2^{2-}] + [T(SH)_2]$. The stability constant for $[Sb(tart)^-]$, K_{tart}, is known ($\log K_{tart} = 14.8$ at 293 K, $I = 0.1$ M) [34]:

Table 3 pM values of selected metal-GSH complexes and the binary complex of $Sb^{III}(TS_2)$

Complex	pM
$Zn^{II}(GS)_2$	6.9
$Cd^{II}(GS)_2$	9.3
$Hg^{II}(GS)_2$	34.6
$Bi^{III}(GS)_3$	26.5
$Sb^{III}(GS)_3$	22.1
$As^{III}(TS_2)$	8.04
$Sb^{III}(TS_2)$	24.5

$$Sb^{III} + tart^{4-} \rightarrow [Sb(tart)^-] \qquad K_{tart} = \frac{[Sb(tart)^-]}{[Sb^{3+}][tart^{4-}]} \qquad (2)$$

Hence the pH^*-dependent stability constant of $[Sb(TS_2)]$ (K'_{TS2}) can be obtained by means of the relationship $K'_{TS2} = K \times K_{tart}$:

$$Sb^{III} + TS_2^{2-} \rightarrow [Sb(TS_2)^+] \qquad K'_{TS_2} = \frac{[Sb(TS_2)^+]}{[Sb^{III}][TS_2^{2-}]} \qquad (3)$$

The pH-independent stability constant (K_{TS2}) can be obtained by assuming the pK_a value of $T(SH)_2$ is 7.40 [35], with an average value of $\log K_{TS2}$ of 23.6 ± 0.4 in 0.1 M $NaNO_3$ (Table 2).

In order to compare the Sb^{III} binding affinity of $T(SH)_2$ with that of arsenic, the pM value was calculated and is listed in Table 3 together with the pM values of metal-glutathione complexes, where $pM = -\log[M]$, and [M] is the concentration of unchelated unhydrolyzed metal ion at equilibrium in a pH 7.4 solution of 1 μM metal and 10 μM ligand.

Discussion

The chemistry of antimony is well known at the molecular level. However, its biological chemistry and molecular pharmacology are poorly understood even though it has been used medicinally for several decades, as are its potential carcinogenic and genotoxic mechanisms [36]. No X-ray crystal structure of antimony and arsenic with biomolecules was available until recently [37]. In contrast to its analogue arsenic, the uptake process of Sb^V into cells and the mechanism of reduction or activation of antimonial drugs still remain unclear. $T(SH)_2$ is the most important low molecular mass thiol (> 80%) inside parasites (e.g., ~5 mM in *Leishmania donovani*) [17], and plays a crucial role in maintenance of cellular redox homeostasis. Elevated cellular $T(SH)_2$ has been reported and found to be related to antimonial resistance in *Leishmania* [21]. The lack of information on the Sb^{III}-trypanothione complex prompted us to investigate the complexation of $T(SH)_2$ to antimonial.

The reduction of arsenate (As^V) to arsenite (As^{III}) in bacteria, yeasts and mammals is catalyzed by the arsenate reductase and has been well documented [7, 8, 9, 10]. In contrast, little is known about the chemical fate of antimonials in trypanosomatids and only a small percentage of Sb^V in human bodies was reduced to Sb^{III} after 12 h [36]. Surprisingly, we found that Sb^V can be reduced to Sb^{III} by $T(SH)_2$ at 310 K and pH 6.4 ($k = 4.42\ M^{-1}\ min^{-1}$, $t_{1/2} = 113 \pm 5$ min), in contrast to its analogue glutathione (days). Interestingly, other reducing dithiols such as DTT were found to reduce Sb^V to Sb^{III} at a comparable rate to GSH, although a better reduction rate ($E^\circ_{1/2} = -0.330$ V) had been expected. This indicates that trypanothione is unique for the reduction (activation) of Sb^V. We should bear in mind that the actual concentration of $T(SH)_2$ inside parasites may remain constantly high because of the presence of a NADPH-dependent TR reducing cycle, and hence a higher reduction rate would be expected in vivo. The reduction process is both pH- and temperature-dependent and favors at an elevated temperature and an acidic pH. Although the intracellular cytosolic pH of both promastigotes and amastigotes is only slightly acidic (pH = 6.5–6.8) [38], promastigotes are known to grow at 298 K while amastigotes are cultured at 310 K [39]. Therefore reduction of antimonials probably occurs at amastigotes (intracellular). These data are in good agreement with two recent reports on the reduction of Sb^V by low molecular thiols [40] and on intracellular antimonial (Sb^V) reduction in *Leishmania donovani*, based on hydride generation-inductively coupled plasma-mass spectrometry (HG-ICP-MS) [6], which showed that the intracellular reduction of Sb^V is a kinetically controlled process. Up to 30% of the Sb^V was reduced to Sb^{III} in amastigotes (310 K) and little reduction of Sb^V to Sb^{III} was observed in promastigotes (299 K) after 12 h. This suggests that trypanothione might play an important role in antimonial activation. However, we cannot exclude the possibility of the presence of an enzyme that catalyzes Sb^V reduction. For example, although As^V is reduced by GSH and other low molecular thiols, this process is too slow and cells use arsenate reductase instead [23, 24]. The reduced Sb^{III} may subsequently bind to trypanothione.

Our ^1H (and ^{13}C) NMR and ESI-MS data show that Sb^{III} forms a stable complex with $T(SH)_2$ with the stoichiometry $Sb^{III}T(S)_2$, and that the trypanothione is bound by deprotonated thiolate sulfurs. This is obvious from a comparison of the Sb^{III}-induced changes of shifts in ^1H NMR spectrum with those of free $T(SH)_2$, which are ~0.38 and 0.13 ppm for the Cys βCH_2 and αCH, respectively, whereas the changes of shifts for other residues of $T(SH)_2$ are not evident. Therefore, the interaction of antimonial (Sb^V) with $T(SH)_2$ involves two steps: reduction and complexation, and each step requires one mol equiv of $T(SH)_2$ and hence the overall reaction can be represented as (H^+ is omitted in the equation):

$$Sb^V + 2T(SH)_2 \rightarrow Sb^{III}(TS_2) + T(S-S) \qquad (4)$$

We suggested earlier, in a brief report, that a water molecule probably binds to the Sb^{III} center, in addition to two thiolate sulfurs from $T(SH)_2$ [41]. Therefore, complex **1** can be represented as $(H_2O)Sb^{III}(TS_2)$, in contrast to its glutathione complex, $Sb^{III}(GS)_3$ [32]. This is probably because the sterically hindered $T(SH)_2$ prevents the third sulfur from an adjacent $T(SH)_2$ from binding to an Sb^{III} center. Both ESI-MS and NMR data indicate that **1** is a monomer with two sulfurs from $T(SH)_2$ and probably an oxygen from a water molecule. This is consistent with the recent crystal structure of an As^{III}/Sb^{III}-translocating ArsA ATPase [37]. In this Sb^{III}-protein complex, a novel Sb^{III} cluster was observed and Sb^{III} interacts with ArsA as a soft metal. Each Sb^{III} coordinates to three donate atoms, two of them from protein residues (e.g., Cys, His or Ser), and the third from a non-protein ligand (probably Cl^-). The S_b–S bond distances are between 2.58 and 2.62 Å, slightly longer than those in $Sb^{III}(SC_6H_2Pr^i_3\text{-}2,4,6)_3$ [42]. Both complex **1** and Sb^{III}-ArsA ATPase could be regarded as an intermediate, and coordination of the non-protein (peptide) ligand may allow it to be readily replaced by other thiols (vide infra).

Complexation of $T(SH)_2$ to the arsenical drug melarsen oxide has been characterized and shown to bind at thiolate sulfurs only [43]. The much larger pM value of **1** compared with the melarsen oxide-trypanothione complex clearly indicates that binding of $T(SH)_2$ to Sb^{III} is much stronger than to As^{III}. Similarly, the affinity of Sb^{III} for $T(SH)_2$ is about 100 times higher than that for GSH, probably due to the chelate effect and slightly lower pK_a value of the thiolate group (~7.4) [35]. This conclusion is also supported by the displacement of either GSH or cysteine by $T(SH)_2$ from $Sb^{III}(GS)_3$ and $Sb^{III}(Cys)_3$ complexes, but not the reverse. The strong binding of Sb^{III} to thiolate sulfur of $T(SH)_2$ suggests that proteins and enzymes are the biological target for Sb^{III} in parasites (and cells).

Surprisingly, the addition of monothiols such as cysteine and GSH results in the formation of a ternary complex. The ternary complex is independent of the order of the binary complex, i.e. either from **1** or $Sb^{III}(GS)_3$ and $Sb^{III}(NAC)_3$. Our ^1H NMR data demonstrated that Sb^{III} in **1** binds to the thiolate group of the ^{13}C-Cys, forming a $(^{13}C\text{-Cys})Sb^{III}(TS_2)$ ternary complex. The formation of the ternary complex indicates that a water molecule initially bound to the Sb^{III} center of the $Sb^{III}(TS_2)$ can readily be displaced by a thiolate group. A ternary complex between proteins (and enzymes) and **1** is thus possible and may account for the biological function of antimony.

In spite of its high thermodynamic stability, complex **1** is kinetically labile toward $T(SH)_2$ exchange. The rate of exchange of $T(SH)_2$ on Sb^{III} is pH dependent, from slow exchange at lower pH (ca. 4) to fast exchange at biological pH. Moreover, exchange between the free and bound ^{13}C-Cys in the ternary complex was also observed (Fig. 5). The presence of minor $Sb(TS_2)_2$ species in the ESI-MS spectrum indicates that it may be an exchange intermediate. $T(SH)_2$ may therefore play an additional role in controlling the free concentration of Sb^{III} in parasites and could perhaps be used as a chaperone to deliver Sb^{III} via thiolates exchange to target proteins and enzymes intracellularly (e.g., trypanothione reductase). Such an exchange of metals (e.g., As^{III} and Cu^I) between thiolate sulfurs has been noted previously for low molecular mass ligands and proteins [44, 45, 46].

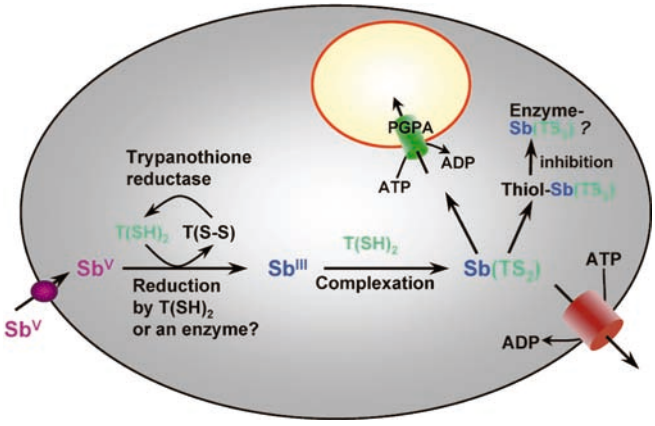

Fig. 6 A proposed mechanism for antimonial in *Leishmania*. The first step is the protein-mediated uptake of Sb^V into parasites. The second step is the intracellular reduction of Sb^V to Sb^{III} by $T(SH)_2$ (or an "enzyme"), and the oxidized trypanothione [T(S-S)] is reduced by trypanothione reductase (TR). The third step involves binding of Sb^{III} to $T(SH)_2$ and is followed by targeting the enzyme via thiolate exchange. Simultaneously, the $Sb^{III}(TS_2)$ complex can be pumped out of cells via an ATP-coupled transporter [20]

We therefore propose a five-step model for the action of antimonials (Fig. 6). The first step involves the uptake of antimonials (Sb^V) into parasites. Our initial results have demonstrated that only Sb^V binds to the iron transport protein lactoferrin rather than Sb^{III}, and the uptake of Sb^V is probably protein mediated (Yan and Sun, unpublished data). The second step is the reduction/activation of Sb^V to Sb^{III} by trypanothione. However, direct interaction of Sb^V with nucleosides at acidic conditions (pH≈5) may also be possible, as suggested recently [47]. The third step involves complexation of Sb^{III} to trypanothione to form $LSb^{III}T(TS_2)$ ($L = H_2O$, Cl^- or other thiol ligands). This is followed by the transfer of Sb^{III} via thiolate exchange and finally targeting proteins or enzymes. Finally, the resistance of parasites to antimonials is due to pumping of the complex $LSb^{III}(TS_2)$ out of cells. An intracellular metal-thiol (As^{III}/Sb^{III}-glutathione/trypanothione) transporter ATPase (PGPA) has been identified in *Leishmania* [20]. Further biological experiments will be needed to confirm the above hypothesis.

Acknowledgements This work was supported by the Research Grants Council of Hong Kong (HKU7110/02P), the University of Hong Kong (UGC) and Hung Hing Ying Physical Sciences Research Fund, and was also partially supported by an Area of Excellence grant. We are grateful to the University of Hong Kong

for a research studentship (to S.Y.), and Profs. A.H. Fairlamb (Dundee, UK) and J.-F. Chiu (HK) for helpful comments.

References

1. Olliaro PL, Bryceson ADM (1993) Parasitol Today 9:323–328
2. Berman JD (1997) Clin Infect Dis 24:684–703
3. Sun H (2002) Metallodrugs. In: Grant DM, Harris RK (eds) Encyclopedia of nuclear magnetic resonance, vol 9: advances in NMR. Wiley, Chichester, pp 413–427
4. Reglinski J (1998) Environmental and medicinal chemistry of arsenic, antimony and bismuth. In: Norman NC (ed) Chemistry of arsenic, antimony and bismuth. Blackie, London, pp 403–440
5. Guo Z, Sadler PJ (2000) Adv Inorg Chem 49:183–306
6. Shaked-Mishan P, Ulrich N, Ephros M, Zilberstein D (2001) J Biol Chem 276:3971–3976
7. Zegers I, Martins JC, Willem R, Wyns L, Messens J (2001) Nat Struct Biol 8:843–847
8. Messens J, Martins JC, Belle KV, Brosens E, Desmyter A, De Gieter M, Wieruszeski J-M, Willem R, Wyns L, Zegers I (2002) Proc Natl Acad Sci USA 99:8506–8511
9. Martin P, DeMel S, Shi J, Gladysheva T, Gatti DL, Rosen BP, Edwards BFP (2001) Structure 9:1071–1081
10. Tamás MJ, Wysocki R (2001) Curr Genet 40:2–12
11. Rosen BP (1999) Trends Microbiol 7:207–212
12. Radabaugh TR, Aposhian HV (2000) Chem Res Toxicol 13:26–30
13. Radabaugh TR, Sampayo-Reyes A, Zakharyan RA, Aposhian HV (2002) Chem Res Toxicol 15: 692–698
14. Messens J, Martins JC, Brosens E, Belle KV, Jacobs DM, Willem R, Wyns L (2002) J Biol Inorg Chem 7:146–156
15. Fairlamb AH, Blackburn P, Ulrich P, Chait BT, Cerami A (1985) Science 227:1485–1487
16. Fairlamb AH (1988) The role of glutathionylspermidine and trypanothione in regulation of intracellular spermidine levels during growth of *Crithidia fasciculata*. In: Zappia, V, Pegg, AE (eds) Progress in polyamine research: novel biochemical, pharmacological and clinical aspects. (Advances in experimental medicine and biology, vol 250) Plenum Press, New York, pp 667–674
17. Fairlamb AH, Cerami A (1992) Ann Rev Microbiol 46:695–729
18. Dumas C, Ouellette M, Tovar J, Cunningham ML, Fairlamb AH, Tamar S, Olivier M, Papadopoulou B (1997) EMBO J 16:2590–2598
19. Tovar J, Cunningham ML, Smith AC, Croft SL, Fairlamb AH (1998) Proc Natl Acad Sci USA 95:5311–5316
20. Légaré D, Richard D, Mukhopadhyay R, Stierhof Y-D, Rosen BP, Haimeur A, Papadopoulou B, Ouellette M (2001) J Biol Chem 276:26301–26307
21. Mukhopadhyay R, Dey S, Xu N, Gage D, Lightbody J, Ouellette M (1996) Proc Natl Acad Sci USA 93:10383–10387
22. Augustyns K, Amssoms K, Yamani A, Rajan PK, Haemers A (2001) Curr Pharm Des 7:1117–1141
23. Scott N, Hatlelid KM, MacKenzie NE, Carter DE (1993) Chem Res Toxicol 6:102–106
24. Delnomdedieu M, Basti MM, Otvos JD, Thomas DJ (1994) Chem Biol Interact 90:135–155
25. Frézard F, Demicheli C, Ferreira CS, Costa MAP (2001) Antimicrob Agents Chemother 45:913–916
26. Mukhopadhyay R, Shi J, Rosen BP (2000) J Biol Chem 275:21149–21157
27. Ellman Gl (1959) Arch Biochem Biophys 82:70–77
28. Piotto M, Saudek V, Sklenar V (1992) J Biomol NMR 2:661–666
29. Burns JA, Butler JC, Moran J, Whitesides GM (19914) J Org Chem 56:2648–2650
30. Rath S, Jardim WF, Dórea JG (1997) Fresenius' J Anal Chem 358:548–550
31. Henderson GB, Glushka J, Cowburn D, Cerami A (1990) J Chem Soc Perkin Trans I 911–914
32. Sun H, Yan S-C, Cheng W-S (2000) Eur J Biochem 267:5450–5457
33. Gress ME, Jacobson RA (1974) Inorg Chim Acta 8:209–21
34. Pettit G, Pettit, LD (1997) IUPAC stability constants database. IUPAC and Academic Software, Otley, UK
35. Moutiez M, Meziane-Cherif D, Aumercier M, Sergheraert C, Tartar A (1994) Chem Pharm Bull 42:2641–2644
36. Gebel T (1997) Chem Biol Interact 107:131–144
37. Zhou T, Radaev S, Rosen BP, Gatti DL (2000) EMBO J 19:4838–4845
38. Marchesini N, Docampo R (2002) Mol Biochem Parasitol 119:225–236
39. Saar Y, Ransford A, Waldman E, Mazareb S, Amin-Spector S, Plumblee J, Turco SJ, Zilberstein D (1998) Mol Biochem Parasitol 95:9–20
40. Ferreira CS, Martins PS, Demicheli C, Brochu C, Ouellette M, Frézard F (2003) Biometals 16:441–446
41. Yan S-C, Ding KY, Zhang L, Sun H (2000) Angew Chem Int Ed 39:4260–4262
42. Bochmann M, Song X, Hursthouse MB, Karaulov A (1995) J Chem Soc Dalton Trans 1649–1652
43. Fairlamb AH, Henderson GB, Cerami A (1989) Proc Natl Acad Sci USA 86:2607–2611
44. Delnomdedieu M, Basti MM, Otvos JD, Thomas DJ (1993) Chem Res Toxicol 6:598–602
45. Wernimont AK, Huffman DL, Lamb AL, O'Halloran TV, Rosenzweig AC (2000) Nat Struct Biol 7:766–771
46. Li S, Rosen BP, Borges-Walmsley MI, Walmsley AR (2002) J Biol Chem 277:25992–26002
47. Demicheli C, Frézard F, Lecouvey M, Garnier-Suillerot A (2002) Biochim Biophys Acta 1570: 192–198